Queensland University of Technology
Brisbane Australia

This may be the author's version of a work that was submitted/accepted for publication in the following source:

Frost, Raymond, Henry, Dermot, Weier, Matthew, & Martens, Wayde (2006)
Raman Spectroscopy of Three Polymorphs of BiVO4: Clinobisvanite, Dreyerite and Pucherite, with Comparisons to (VO4)3- Bearing Minerals: Namibite, Pottsite and Schumacherite.
Journal of Raman Spectroscopy, *37*(7), pp. 722-732.

This file was downloaded from: https://eprints.qut.edu.au/225081/

© Consult author(s) regarding copyright matters

This work is covered by copyright. Unless the document is being made available under a Creative Commons Licence, you must assume that re-use is limited to personal use and that permission from the copyright owner must be obtained for all other uses. If the document is available under a Creative Commons License (or other specified license) then refer to the Licence for details of permitted re-use. It is a condition of access that users recognise and abide by the legal requirements associated with these rights. If you believe that this work infringes copyright please provide details by email to qut.copyright@qut.edu.au

Notice: *Please note that this document may not be the Version of Record (i.e. published version) of the work. Author manuscript versions (as Submitted for peer review or as Accepted for publication after peer review) can be identified by an absence of publisher branding and/or typeset appearance. If there is any doubt, please refer to the published source.*

https://doi.org/10.1002/jrs.1499

COVER SHEET

Frost, Ray and Henry, Dermot and Weier, Matt and Martens, Wayde (2006) Raman spectroscopy of three polymorphs of BiVO4: clinobisvanite, dreyerite and pucherite, with comparisons to (VO4)3-bearing-minerals: namibite, pottsite and schumacherite. ***Journal of Raman Spectroscopy*** **37(7):pp. 722-732.**

Copyright 2006 John Wiley & Sons.

Accessed from: http://eprints.qut.edu.au/archive/00004763

Raman spectroscopy of three polymorphs of BiVO4: clinobisvanite, dreyerite and pucherite, with comparisons to $(VO_4)^{3-}$-bearing minerals: namibite, pottsite and schumacherite

Ray L. Frost[•a], Dermot A. Henry[b], Matt L. Weier [a] and Wayde Martens [a]

[a] Inorganic Materials Research Program, School of Physical and Chemical Sciences, Queensland University of Technology, GPO Box 2434, Brisbane Queensland 4001, Australia.

[b] Museum Victoria, Geosciences, GPO Box 666E , Melbourne. Victoria. Australia 3001

Abstract

Both Raman and infrared spectroscopy have been used to characterise the three phase related minerals dreyerite (tetragonal $BiVO_4$), pucherite (orthorhombic $BiVO_4$) and clinobisvanite (monoclinic $BiVO_4$) and a comparison of the spectra is made with that of the minerals namibite ($Cu(BiO_2)VO_4(OH)$), schumacherite ($(Bi_3O(OH)(VO_4)_2$) and pottsite ($PbBiH(VO_4)_2.2H_2O$) . Pucherite, clinobisvanite and namibite are characterised by VO_4 stretching vibrations at 872, 824 and 846 cm^{-1}. The Raman spectrum of dreyerite shows complexity in the 750 to 950 cm^{-1} region with two intense bands at 836 and 790 cm^{-1} assigned to the symmetric and antisymmetric VO_4 modes. The minerals schumacherite and pottsite are characterised by bands at 846 and 874 cm^{-1}. In both the infrared and Raman spectra bands are observed in the 1000- 1100 cm^{-1} region which are attributed to the antisymmetric stretching modes. The Raman spectra of the low wavenumber region are complex. Bands are identified in the 328 to 370 cm^{-1} region and in the 404 to 498 cm^{-1} region and are assigned to the ν_2 and ν_4 bending modes. The minerals namibite and schumacherite are characterised by intense bands at 3514 and 3589 cm^{-1} assigned to the symmetric stretching vibrations of the OH units. Importantly Raman spectroscopy enables new insights into the chemistry of these bismuth vanadate minerals. Raman

• Author for correspondence (r.frost@qut.edu.au)

spectroscopy enables the identification of the bismuth vanadate minerals in mineral matrices where paragenetic relationships exist between the minerals.

Keywords: pucherite, namibite, schumacherite, clinobisvanite, dreyerite, vanadates, Raman spectroscopy, infrared spectroscopy

Introduction

Very little published data exists on the Raman spectra for minerals which contain $(VO_4)^{3-}$. [1] There are approximately 70 minerals which contain $(VO_4)^{3-}$ groups. [2] In basic pH conditions these form simple structures with VO_4 tetrahedra but with increasing acidity these tetrahedra link into chains and then into polynuclear groups of square pyramids or distorted octahedra. [3] Interest in the minerals arises from their ferroelectric properties. Raman spectroscopy has been used to determine the ferroelastic - paraelastic phase transition in tetragonal $BiVO_4$. [4]

Bismuth vanadates can be readily synthesised [5] and modified through grinding. [6] Such syntheses are useful for preparing ferroelectric materials. [7] Crystal structures are stable even under high pressure. [8] A ferroelastic, tetragonal-to-monoclinic phase transition at 525 K was confirmed. [9] Such materials have the potential for photo catalytic activity such as for the photocatalysis of water. [10] The monoclinic $BiVO_4$ showed high photocatalytic activity. Distortion of a Bi-O polyhedron by a 6s2 lone pair of Bi^{3+} plays an important role for high photocatalytic activity of the monoclinic $BiVO_4$ under visible light irradiation. [10] It was found that Tetragonal $BiVO_4$ with a 2.9 eV band gap mainly possessed an UV absorption band while monoclinic $BiVO_4$ with a 2.4 eV band gap had a characteristic visible light absorption band in addition to the UV band. [11,12]

This paper will examine the Raman spectra for the three naturally occurring polymorphs of $BiVO_4$: clinobisvanite, dreyerite, and pucherite and compare with the spectra of bismuth-bearing minerals containing tetrahedral vanadium: namibite ($Cu(BiO_2)VO_4(OH)$), pottsite ($PbBiH(VO_4)_2.2H_2O$) and schumacherite ($Bi_3O(OH)(VO_4)_2$).

THE MINERALS

The minerals studied in this research are given in Table 1.

Pucherite

Pucherite, orthorhombic $BiVO_4$, was the first described polymorph and is the most widespread. Initially described from the Pucher shaft, Wolgang Massen mine near Schneeberg, Germany. [13] It has subsequently been discovered in oxidised ores in a variety of geological settings and in zoned pegmatites. It is recorded from over 20 localities worldwide. [2] The mineral is polymorphic with clinobisvanite and dreyerite. The structure of pucherite was initially determined by [14-16] and subsequently refined by Fischer *et al.,* 1958. [17] It is orthorhombic, space group Pnca, with a 5.328(2), b 5.052(2), and c 12.003(3) Å at 291 K; d.(calcd.) = 6.69 for Z = 4. The structure consists of VO_4 tetrahedra and BiO_8 triangulated dodecahedra. Each dodecahedron shares 1 edge with a tetrahedron and 2 edges with neighbouring dodecahedra. Synthetically, pucherite will convert to a monoclinic form above 500 °C. [18]

Clinobisvanite

Clinobisvanite, monoclinic $BiVO_4$, was initially described from a pegmatite, 5 km south of Pyramid Hill, Yinnietharra Station. [19] Clinobisvanite occurs as an accessory mineral in pegmatites as an oxidation product of other bismuth minerals and is recorded from about 17 localities world wide. [2] The crystallographic data for clinobisvanite has been determined on synthetic material as monoclinic, space group I2/a, with a = 5.195, b = 11.701, c = 5.092 Å and β = 90.38°. [20] Clinobisvanite may convert to the tetragonal form (dreyerite). [21,22] This is the ferroelastic monoclinic-tetragonal phase transition in $BiVO_4$. Supergene clinobisvanite which has replaced supergene dreyerite has been recorded from Lively's gold mine, South Australia. [23]

Dreyerite

The tetragonal polymorph of $BiVO_4$, dreyerite, is known from only one locality near Hirschhorn, near Kaiserlautern, Germany where it occurs in rhyolitic tuffs. [24] The structure of dreyerite was determined on specimens from the type locality as tetragonal, space group,$I4_1/amd$ a = 7.303 (3) c= 6.584(3). [24]

Namibite

Namibite ($Cu(BiO_2)VO_4(OH)$) occurs as a secondary mineral in bismuth-bearing deposits. Initially described from Khorixas, Namibia. [25] Namibite has been described from 12 localities world wide. [26] The single crystal structure of namibite, $Cu(BiO)_2VO_4(OH)$ has been determined to be triclinic, space group P1, with a = 6.210(1), b = 7.398(1), c = 7.471(1) Å . α. = 90.10(1), .β. = 108.73(1), γ. = 107.47(1).degrees, V = 308.22(8) .ANG.3, Z = 2 [27]. The structure determination showed namibite to be triclinic-pseudomonoclinic; the previously reported C-centred monoclinic cell is a pseudocell. The structure contains two unique Bi atoms, with nine Bi-O bonds between 2.17 and 3.39 Å. A three-dimensional network is formed by linkages of Bi-O polyhedra to one slightly distorted $V^{5+}O_4$ tetrahedron that decorates chains of corner-sharing CuO_6 polyhedra extending parallel to the b axis. The CuO_6 polyhedra show the Jahn-Teller-distorted [4+2]-coordination of Cu^{2+}. Layers of Bi atoms parallel to (100) alternate with layers of parallel heteropolyhedral $[Cu(VO_4)O_2(OH)]$ chains. According to bond-valence calculations and geometrical considerations, the H atom of the OH group is probably involved in disordered or trifurcated H bonding. [27]

Pottsite

Pottsite ($PbBiH(VO_4)_2.2H_2O$) is a rare mineral known only from the type locality at the Linka mine, Spencer Hot Springs district, Lander Co, near Potts, Nevada, USA. [28] Pottsite is tetragonal, space group $I4_122$, a = 11.084, c = 12.634 Z = 10.

Schumacherite

Schumacherite ($Bi_3O(OH)(VO_4)_2$) is a rare mineral which occurs in oxidised zones of bismuth-bearing deposits. First recorded from Schneeberg, Germany [29] is only known from only seven localities world wide. Schumacherite is triclinic with space group P1, a = 10.05(3), b = 7.46 (3) c = 6.90(3), α = 87.7(3), , β = 115.3, γ = β and Z = 2. [29] Schumacherite forms a series with the arsenate analogue, priesingerite, and the phosphate equivalent, petitjeanite. [30]

Spectroscopy

The infrared spectra of selected minerals containing pentavalent vanadium have been published by Farmer [31]. There are four vibrations for $(VO_4)^{3-}$, namely the A_1 symmetric stretching mode observed at around 824 cm^{-1}, the E bending mode in the region between 305 and 345 cm^{-1}, the F_2 antisymmetric stretching mode between 780 and 855 cm^{-1} and the F_2 bending mode between 340 and 345 cm^{-1}. The F_2 modes are both Raman and infrared active whereas the A_1 and E modes are Raman active only. The significance of the latter is that infrared spectroscopy will not see all the vibrational modes and vital spectroscopic information is lacking as may be observed in the tables reported by Farmer. [31] Some variation in the table given by Farmer is noted. S.D. Ross in Chapter 17 of Farmer shows a table of the fundamental vibrational frequencies of the tetrahedral anions with pentavalent central atoms. The A_1 symmetric stretching modes are observed at around 824 cm^{-1} or around 870 to 874 cm^{-1}. The F_2 antisymmetric stretching mode varied between 780 and 855 cm^{-1}. In general the antisymmetric stretching mode occurred at wavenumbers below that of the symmetric stretching mode. The E bending mode in the region was found between 305 and 340 cm^{-1} and the F_2 bending mode between 340 and 345 cm^{-1}. It is apparent that both the F_2 and E bending modes occur at similar positions. In aqueous systems of the pentavalent vanadate ion, the bands are found at 874, 345, 855 and 345 cm^{-1} [32,33]. Farmer also reported the infrared bands of pucherite. The ν_1 symmetric stretching modes were observed at 825 and 808 cm^{-1}, the ν_2 bending modes at 475, 423 and 405 cm^{-1} and the ν_4 bending modes at 610 cm^{-1}. Some Raman spectra of selected vanadates have been forthcoming. [1] Raman spectroscopy has been applied to the study of the mixed oxides of vanadium and to mixed metal bismuthates-vanadates. [34,35]

Experimental data

Samples

The minerals in Table 1 were obtained from Museum Victoria and were analysed by electron probe for chemical composition and by X-ray powder diffraction for phase identification where sufficient material was available. Raman spectroscopy was utilised to confirm the identification of pucherite from Morass Creek, Victoria, Australia described by Birch et al, 1995. [36]

Raman microprobe spectroscopy

Raman spectroscopy has proven very useful for the study of minerals which show common paragenesis. The technique enables the spectra to be obtained in situ without any sample preparation other than the alignment of the samples in the incident beam. The crystals of the bismuth vanadate minerals were placed and orientated on the stage of an Olympus BHSM microscope, equipped with 10x and 50x objectives and part of a Renishaw 1000 Raman microscope system, which also includes a monochromator, a filter system and a Charge Coupled Device (CCD). Raman spectra were excited by a HeNe laser (633 nm) at a resolution of 2 cm^{-1} in the range between 100 and 4000 cm^{-1}. Repeated acquisition using the highest magnification was accumulated to improve the signal to noise ratio. Spectra were calibrated using the 520.5 cm^{-1} line of a silicon wafer. In order to ensure that the correct spectra are obtained, the incident excitation radiation was scrambled. Previous studies by the authors provide more details of the experimental technique. Spectra at controlled temperatures were obtained using a Linkam thermal stage (Scientific Instruments Ltd, Waterfield, Surrey, England). Details of the technique have been published by the authors [32,37-41]. Spectral manipulation such as baseline adjustment, smoothing and normalisation was performed using the GRAMS® software package (Galactic Industries Corporation, Salem, NH, USA).

Infrared spectroscopy

Infrared absorption spectra were obtained using the KBr pressed pellet technique using a Perkin-Elmer FT-IR spectrometer 2000 bench using 4 cm^{-1} resolution with 128 scans. Infrared spectra were obtained using a Nicolet Nexus 870 FTIR spectrometer with a smart endurance single bounce diamond ATR cell. Spectra over the 4000–525 cm^{-1} range were obtained by the co-addition of 64 scans with a resolution of 4 cm^{-1} and a mirror velocity of 0.6329 cm/s. Spectra were co-added to improve the signal to noise ratio.

RESULTS AND DISCUSSION

Factor group analysis

The single crystal studies of several of the minerals included in this study have not been published. The reason may be attributed to the lack of useable crystals for this type of study. Only the single crystal studies of pucherite, clinobisvanite and namibite have been forthcoming.

Pucherite

The mineral pucherite is orthorhombic with z=4.

The following table shows the factor group analysis for the VO_4 unit

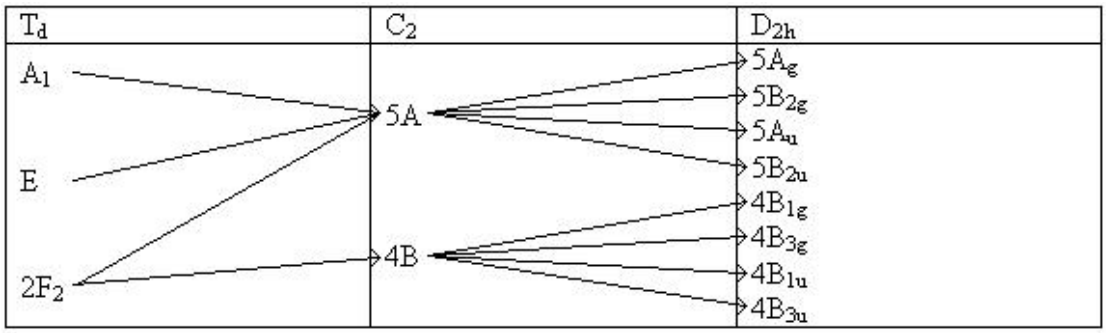

$\Gamma_{lattice} = 3A_g + 6B_{1g} + 3B_{2g} + 6B_{3g} + 3A_u + 2B_{2u} + 5B_{1u} + 5B_{3u}$

All g modes Raman active; B_{2u}, B_{1u}, B_{3u} modes Infrared active; A_u modes inactive. Thus there are 36 internal vibrations associated with the vanadate ion. The FGA shows that there will be two symmetric Raman active modes the A_g and B_{2g}. The A_u mode will be inactive and the B_{2u} mode will be infrared active only. FGA shows there will be six Raman active antisymmetric stretching modes A_g, B_{2g}, $2B_{1g}$, and $2B_{3g}$. For the antisymmetric stretching modes, the infrared active vibrations are B_{2u}, $2B_{1u}$ and $2B_{3u}$.

Clinobisvanite

The mineral clinobisvanite is monoclinic with z=4.

The following table shows the factor group analysis for the VO_4 unit

$\Gamma_{lattice} = 3A_g + 2A_u + 6B_g + 4B_u$

All g modes are Raman active; All u modes are IR active. Thus there will be 18 internal vibrations. The Raman active modes will be the A_g and B_g modes.

Namibite

The mineral namibite is triclinic with z= 2.

The following table shows the factor group analysis for the VO_4 unit

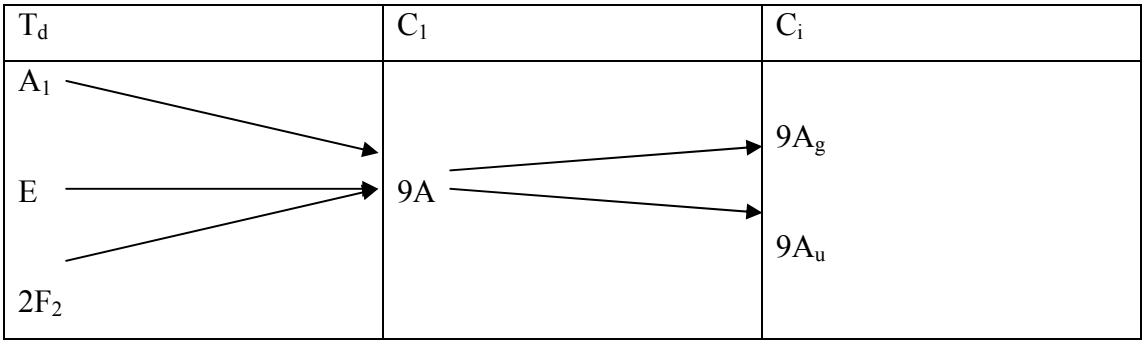

$\Gamma_{lattice} = 27A_u + 24A_g$

All g modes Raman Active. All u modes IR active.

Raman spectroscopy of the bismuth vanadates

A number of problems arise when natural vanadates of bismuth are studied. Firstly isomorphic substitution may occur such as replacement of the vanadate by

phosphate, sulphate or even arsenate. The mineral schumacherite from Wombat Hole Prospect, Morass Creek gorge, near Benambra, Victoria, Australia shows both the presence of phosphate and arsenate at low concentrations. Further in some samples some low concentration cationic substitution can occur. For example the analysis of clinobisvanite from the Londonderry quarry, near Coolgardie, Western Australia shows the presence of both Pb and Ca. This will result in the observation of additional bands which do not belong to the $BiVO_4$ mineral. Secondly the minerals have close paragenetic relationships. In other words crystals of the minerals may be adjacent to each other and care must be taken when characterising the minerals by Raman spectroscopy. Selection of the BiO4 crystal is made according to the crystal shape of the mineral. Thirdly because the samples are exposed to soils adsorbed organics and adsorbed water may be present in the samples. The sample of pucherite (M48584) from The Wombat Hole prospect, Morass Creek Gorge shows from the infrared spectrum, the presence of water and other minerals in the sample. The pucherite mineral (M5512) from Germany shows also from the infrared spectrum the presence of organics associated with the mineral. These impurities are not as obvious in the Raman spectra. This no doubt is because both the adsorbed water and the organic impurities are very poor Raman scatterers.

The Raman spectra of the 750 to 950 cm^{-1} region of the series of minerals listed above are shown in Figure 1. The results of the band component analyses of the Raman and infrared spectra of selected minerals shown in Table 1 are reported in Tables 2 and 3. The mineral pucherite is characterised by a symmetric bands at 872 and 881 cm^{-1}. The observation of two bands is in agreement with the prediction of the factor group analysis which predicted two bands attributed to symmetric stretching modes. Clinobisvanite are characterised by a single band at 828 cm^{-1} attributed to the ν_1 symmetric stretching mode in harmony with the FGA which predicted a single band. Namibite is characterised by a single symmetric stretching band at 846 cm^{-1}. FGA also predicts a single symmetric stretching vibration.

Farmer gave the position of the A_1 symmetric stretching mode for pucherite as 825 cm^{-1}. [31] The Raman spectrum of dreyerite shows complexity in the 750 to 950 cm^{-1} region with two intense bands at 836 and 790 cm^{-1} attributed to the ν_1 symmetric stretching mode and the ν_3 antisymmetric stretching mode. [42,43] Thus the three

minerals are readily identified by the position of the symmetric stretching modes. The Raman spectrum of schumacherite shows an intense band at 846 cm^{-1}. For completeness the Raman spectrum of pottsite ($HPbBi(VO_4)_2.2H_2O$) is included. This mineral shows an intense band at 874 cm^{-1}. The crystal structures of schumacherite and pottsite are not known and hence the factor group analysis could not be undertaken. The Raman spectrum of pottsite shows asymmetry on the high wavenumber side. This suggests two symmetric stretching modes.

The Raman spectra of the 250 to 750 cm^{-1} region for the selected vanadate minerals of bismuth are shown in Figure 2. The most intense bands are found in the 308 to 370 cm^{-1} region. The Raman spectrum of dreyerite displays three bands at 365, 321 and 301 cm^{-1}. The Raman spectra of pucherite (M5512) show two bands at 346 and 333 cm^{-1}. The second pucherite (M48584) sample shows bands at 336 and 308 cm^{-1}. These bands are attributed to the ν_2 symmetric bending modes of the VO_4 units. FGA for pucherite predicts 10 bands in the region from 300 to 500 cm^{-1}. It is possible to put this many bands in the spectral profile using band fitting. However it is questionable that the bands are placed in the correct positions.

The spectra of clinobisvanite show bands at around 365 and 333 cm^{-1} and are described as the ν_2 bending modes of the VO_4 units. Farmer described the ν_2 (*E*) bending mode of the VO_4 units in the region 305 and 345 cm^{-1}. This attribution fits well with the data found this work. Farmer also attributed the ν_4 (F_2) bending mode between 340 and 345 cm^{-1}. Thus an alternative assignation would be to describe the band for pucherite at 346 cm^{-1} as the ν_4 mode and the band at 333 cm^{-1} as the ν_2 mode. However in all of the spectra intense bands are observed in the 370 to 475 cm^{-1} region and it is proposed that these bands are more readily assigned to the ν_4 out-of-plane bending modes. The Raman spectrum of dreyerite shows two intense overlapping bands at 452 and 462 cm^{-1}. Farmer listed three bands in these positions at 475, 423 and 405 cm^{-1}. The Raman spectrum of the mineral pottsite shows three bands at 370, 348 and 331 cm^{-1} assigned to the ν_2 bending modes and three bands at 465, 413 and 404 cm^{-1}. A significant number of bands are found below 300 cm^{-1}. At this stage, the bands are simply described as lattice modes.

Raman and infrared spectra HOH-stretching region

The Raman spectra of the water HOH stretching region is shown in Figure 3. The Raman spectra of dreyerite, pucherite and clinobisvanite should show no bands in the hydroxyl stretching region. Two bands are observed at 3566 and 3478 cm^{-1} for the pucherite sample (M48584). These bands are ascribed to adsorbed water. An alternative assignment is that the observation of bands in this spectral region may be attributed to impurities. This is not unexpected since there are paragenetic relationships between the pucherite minerals. Four clinobisvanite samples show no bands in the Raman spectrum in this spectral region. The infrared spectra of pucherite (M5512) show no bands in the 3000 to 4000 cm^{-1} region (Figure 4). A series of bands are observed at 2917, 2904, 2848 and 2817 cm^{-1}. These bands are assigned to organic impurities, probably adsorbed on the surface. Pucherite sample M48584 shows a series of low intensity bands at 3632, 3562, 3545, 3414 and 3227 cm^{-1}. The infrared spectrum of clinobisvanite (M47276) shows no bands. The other samples of clinobisvanite show bands in the 3305 to 3643 cm^{-1} region. Again it is suggested these bands are due to impurities in the minerals.

The Raman spectrum of namibite (M48585) displays two bands at 3617 and 3514 cm^{-1} (Figure 3). The mineral has the formula ($Cu(BiO_2)VO_4(OH)$); thus the intense band at 3617 cm^{-1} is assigned to the symmetric stretching vibration of these OH units. A series of low intensity bands are observed at around 2912 cm^{-1} and are ascribed to organic impurities adsorbed on the surface of the mineral. The infrared spectrum shows more intensity with a complex set of overlapping bands. Four bands are observed for sample (M48585) at 3623, 3582, 3446 and 3225 cm^{-1}. The first two bands align with the two Raman bands and the latter two bands are attributed to adsorbed water. The Raman spectrum of the mineral schumacherite ($Bi_3O(OH)(VO_4)_2$) shows a single intense band at 3589 cm^{-1} with a shoulder at 3589 cm^{-1}. The infrared spectrum of schumacherite shows four bands at 3618, 3566, 3466 and 3256 cm^{-1}. Both the infrared and Raman spectra of namibite and schumacherite show strong resemblances. In many ways this is not unexpected. The Raman spectrum of pottsite ($HPbBi(VO_4)_2.2H_2O$) displays no Raman bands in the OH stretching region. The infrared spectrum does show bands at 3695, 3648, 3621, 3604 and 3400 cm^{-1}.

Infrared spectra

The infrared spectra of the selected minerals of formula $BiVO_4$ and related minerals are shown in Figure 5. An intense band is observed in the infrared spectra at 1006 cm^{-1} for pucherite with other bands observed at 1229, 1155, 1094, 1060 and 1033 cm^{-1} of significantly lower intensity. These bands are assigned to the ν_3 antisymmetric stretching vibrations of the VO_4 units. A low intensity band is also observed in the Raman spectra at around 1002 cm^{-1} and is also assigned to this vibrational mode. The second pucherite sample (M48584) showed intense bands at 1020 and 1103 cm^{-1}. In the Raman spectrum of dreyerite a strong band is observed at 987 cm^{-1}. Other bands of much less intensity are observed at 1164, 1137, 1104 and 1082 cm^{-1}. These bands are also assigned to the ν_3 antisymmetric stretching vibrations of the VO_4 units. It was not possible to obtain the infrared spectrum of dreyerite because of the rarity of the mineral and the fact that the mineral was borrowed and had to be returned. The mineral namibite shows bands in similar positions at 1006 and 1104 cm^{-1}. The infrared spectrum of the mineral clinobisvanite shows more complexity in the antisymmetric stretching region. Infrared bands are observed around 1036, 1073 and 1163 cm^{-1}. Some sample variation in the peak position is observed. In the Raman spectrum of clinobisvanite, two bands are observed at 1190 and 1280 cm^{-1} and are also attributed to the ν_3 antisymmetric stretching modes. The infrared spectrum of pottsite showed two bands at 1006 and 1105 cm^{-1} ascribed to the ν_3 antisymmetric stretching vibrations. Farmer gave the F_2 antisymmetric stretching mode as between 780 and 855 cm^{-1}. The position of these bands does not match with our data. The Raman spectrum of schumacherite displays bands at 1041 cm^{-1}; pottsite at 1006 and 1105 cm^{-1}. In the infrared spectrum of schumacherite bands are observed at 1171, 1026 and 1000 cm^{-1}; for pottsite bands are observed at 1105 and 1006 cm^{-1}. These bands are assigned to the ν_3 antisymmetric stretching vibrations.

CONCLUSIONS

The minerals pucherite, clinobisvanite, namibite, schumacherite and pottsite have been studied using a combination of Raman and infrared spectroscopy. Raman spectroscopy enables the minerals to be analysed in situ without any sample

preparation. Only the alignment and focussing of the mineral is required. The minerals listed above can be readily distinguished simply by the position of the VO_4 symmetric stretching vibration. Raman spectroscopy is a very powerful technique for studying minerals which form thin films on a host matrix. Particularly when only a very small amount of material is available, which may be insufficient for X-ray diffraction studies, (eg Morass Creek material).

Vibrational spectroscopy enables bands to be assigned to the various modes of the VO_4 anion. Bands attributed to OH and water units are observed. . Importantly Raman spectroscopy enables the identification of the bismuth vanadate minerals in mineral matrices where paragenetic relationships exist between the minerals.

Acknowledgements

The financial and infra-structure support of the Queensland University of Technology Inorganic Materials Research Program of the School of Physical and Chemical Sciences is gratefully acknowledged. The Australian Research Council (ARC) is thanked for funding. Museum Victoria is thanked for the loan of the minerals.

References

1. Frost, RL, Erickson, KL, Weier, ML. *Spectrochimica Acta, Part A: Molecular and Biomolecular Spectroscopy* 2004**; 60**: 2419.
2. Anthony JW, Bideaux RA, KW, B, MC, N *Handbook of Mineralogy Volume IV arsenates, phosphates and vanadates.*; Mineral Data Publishing, Tuscon, Arizona, USA, 2000., 2000; Vol. IV.
3. Evans, HT, Jr., White, JS, Jr. *Mineralogical Record* 1987**; 18**: 333.
4. Jang, MS, Park, HL, Kim, JN, Ro, JH, Park, YH. *Japanese Journal of Applied Physics, Part 1: Regular Papers, Short Notes & Review Papers* 1985**; 24**: 506.
5. Gottlieb, IM, Kelly, DP. *Therm. Anal., Proc. Int. Conf., 4th* 1975**; 1**: 675.
6. Bhattacharya, AK, Mallick, KK, Hartridge, A. *Materials Letters* 1997**; 30**: 7.
7. Hazen, RM, Mariathasan, JWE. *Science (Washington, DC, United States)* 1982**; 216**: 991.
8. Mariathasan, JWE, Hazen, RM, Finger, LW. *Phase Transitions* 1986**; 6**: 165.
9. Waskowska, A, Pietraszko, A, Lukaszewicz, K. *Ferroelectrics* 1988**; 79**: 131.
10. Tokunaga, S, Kato, H, Kudo, A. *Chemistry of Materials* 2001**; 13**: 4624.
11. Kudo, A, Omori, K, Kato, H. *Journal of the American Chemical Society* 1999**; 121**: 11459.
12. Kudo, A. Soft-process synthesis of bismuth vanadate. In *Jpn. Kokai Tokkyo Koho*; (Foundation for Scientific Technology Promotion, Japan). Jp, 2001; pp. 5 pp.
13. Frenzel, G. *Neues Jahrbuch fuer Mineralogie, Abhandlungen* 1971**; 115**: 164.
14. Fischer, E, Kleber, W, Sommer, J. *Chemie der Erde* 1958**; 19**: 361.
15. Qurashi, MM, Barnes, WW. *American Mineralogist* 1953**; 38**: 489.
16. Qurashi, MM, Barnes, WH. *American Mineralogist* 1952**; 37**: 423.
17. Granzin, J, Pohl, D. *Zeitschrift fuer Kristallographie* 1984**; 169**: 289.
18. Roth, RS, Waring, JL. *American Mineralogist* 1963**; 48**: 1348.
19. Bridge, PJ, Pryce, MW. *Mineralogical Magazine* 1974**; 39**: 847.
20. Swanson, HE, Morris, MC, Evans, EH, Ulmer, L. *NBS Monograph (United States)* 1964**; Monograph 25**: 64 pp.
21. Wood, IG, Welber, B, David, WIF, Glazer, AM. *Journal of Applied Crystallography* 1980**; 13**: 224.

22. Wood, IG, Glazer, AM. *Journal of Applied Crystallography* 1980**; 13**: 217.
23. Collier, JB, Plimer, IR. *Neues Jahrbuch fuer Mineralogie, Monatshefte* 2002: 401.
24. Dreyer, G, Tillmanns, E. *Neues Jahrbuch fuer Mineralogie, Monatshefte* 1981: 151.
25. Von Knorring, O, Sahama, TG. *Schweizerische Mineralogische und Petrographische Mitteilungen* 1981**; 61**: 7.
26. Dunning, GE, Cooper, JF, Jr. *Mineralogical Record* 1998**; 29**: 163.
27. Giester, G. *American Mineralogist* 2000**; 85**: 1298.
28. Williams, SA. *Mineralogical Magazine* 1988**; 52**: 389.
29. Walenta, K, Dunn, PJ, Hentschel, G, Mereiter, K. *TMPM, Tschermaks Mineralogische und Petrographische Mitteilungen* 1983**; 31**: 165.
30. Krause, W, Belendorff, K, Bernhardt, HJ, Bochum. *Neues Jahrbuch fuer Mineralogie, Monatshefte* 1993: 487.
31. Farmer, VC *Mineralogical Society Monograph 4: The Infrared Spectra of Minerals*, 1974.
32. Frost, RL, Crane, M, Williams, PA, Kloprogge, JT. *Journal of Raman Spectroscopy* 2003**; 34**: 214.
33. Frost, RL, Williams, PA, Kloprogge, JT, Leverett, P. *J. Raman Spectrosc.* 2001**; 32**: 906.
34. Hirata, T, Watanabe, A. *Journal of Solid State Chemistry* 2001**; 158**: 264.
35. Mindel'man, NK, Perelyaeva, LA, Khodos, MY, Zhuravlev, VD. *Zhurnal Neorganicheskoi Khimii* 1990**; 35**: 993.
36. Birch, WD, Henry, DA, Pring, A. *Mineralogical Record* 1995**; 26**: 107.
37. Frost, RL, Williams, PA, Martens, W. *Mineralogical Magazine* 2003**; 67**: 103.
38. Martens, W, Frost, RL, Kloprogge, JT. *Journal of Raman Spectroscopy* 2003**; 34**: 90.
39. Martens, W, Frost, RL, Kloprogge, JT, Williams, PA. *Journal of Raman Spectroscopy* 2003**; 34**: 145.
40. Frost, RL, Martens, W, Kloprogge, JT, Williams, PA. *Journal of Raman Spectroscopy* 2002**; 33**: 801.
41. Frost, RL, Martens, W, Williams, PA, Kloprogge, JT. *Mineralogical Magazine* 2002**; 66**: 1063.

42. Artuso, F, Picardi, G, Bonino, F, Decker, F, Bencic, S, Surca Vuk, A, Opara Krasovec, U, Orel, B. *Electrochimica Acta* 2001**; 46**: 2077.
43. Harley, RT, Hayes, W, Smith, SRP. *Journal of Physics C: Solid State Physics* 1972**; 5**: 1501.

Pucherite	M5512	$BiVO_4$	Pucher shaft, Schneeberg, Germany
Pucherite	M48584	$BiVO_4$	Wombat Hole Prospect, Morass Creek gorge, near Benambra, Victoria, Australia
Clinobisvanite	M47276	$BiVO_4$	Lively's Gold mine Arkaroola, South Australia
Clinobisvanite	M44380	$BiVO_4$	Londonderry Feldspar Quarry, Coolgardie area, Western Australia
Clinobisvanite	M44424	$BiVO_4$	Linka mine, near Spencer Hot Springs, Lander County, Nevada, USA
Dreyerite		$BiVO_4$	Hirschhorn, near Kaiserlautern, Germany
Namibite	M43947	$Cu(BiO_2)VO_4(OH)$	Lodi No.4 mine, Plumas Co. California, USA
Namibite	M48585	$Cu(BiO_2)VO_4(OH)$	Wombat Hole Prospect, Morass Creek gorge, near Benambra, Victoria, Australia
Schumacherite	M48586	$Bi_3O(OH)(VO_4)_2$	Wombat Hole Prospect, Morass Creek gorge, near Benambra, Victoria, Australia
Pottsite	M45004	$(Pb,Bi,H)(VO_4)_2H_2O$	Las Tapias, Cordoba Province, Argentina

Table 1 Samples, museum reference and origin of the $BiVO_4$ samples

Table2 Results of the Raman and infrared spectral analysis of pucherite and clinobisvanite.

Pucherite					Clinobisvanite										Suggested assignments
M5512		M48584			M44424-c		M31828		M44380		M47276		M44424-a		
Raman	IR	Raman	IR	IR published [31]	Raman	IR	Raman	IR	Raman	IR	Raman	IR	Raman	IR	
		3566 3478	3632 3562 3545 3414 3227			3362 3284		3551 3315		3643 3579 3510 3305			3524 3381	3347	Adsorbed water Impurities Due to other minerals
	2917 2904 2848 2817		3092			3106 2919				3097 2925 2902		3191 3086 2919		2919	Organic impurities
		1606	1644 1627					1641		1640				1683	Water HOH deformation modes

	1308	1302						1396		1446		1459 1389 1315		1448	Organic impurities
1002	1229 1155 1094 1060 1033 1006	1002	1103 1020			1163 1073 1036	1280 1190	1148 1097 1035		1096 1048 1007		1206 1110 1031		1027	
881			998 919		882	989 946		989		955 896		891	921 913 909 885		
872	849	872			827 822	832 789	828	849 786	828			872 844 817	840 826 798	854 791	ν_1 symmetric stretching mode of VO_4
	803		818 787	825 808	724	722	723	757 742 722 711 648	756 712	727 680	704	734		726	ν_3 antisymmetric stretching mode of VO_4
710 693	675	665				647									

647															
	591	605		610			625	608 587			610			627	BiO stretching vibration
		516			431		509				451 436		403		ν_4 bending modes of VO_4 units
415 372		439 388		475 423 405	365 333		369 330		368 329		376		365 334 331		ν_2 bending modes of VO_4 units
346 333		336 308													ν_2 bending modes of VO_4 units
					266		293 271 251		245		279		275		Lattice modes
256 224 196 188		229			211		232 215 209 186 170		211 185 167		235 206		231 212 199		Lattice modes

Table 3 Results of the Raman and infrared spectral analysis of namibite, schumacherite and pottsite.

Namibite			Schumacherite		Pottsite		Suggested assignments
M43947	M48585		M48586		M45004		
Raman	Raman	IR	Raman	IR	Raman	IR	
	3617 3514	3623 3582 3446 3255	3616 3589	3618 3566 3446 3256		3695 3648 3621 3604 3400	OH stretching vibrations of OH units and water
	2912	2948		2978	2912		Organic impurities
		1669 1633	1557	1634			Water HOH deformation modes
						1439 1389 1347	Impurity due to the presence of organics

		1104 1006	1041	1171 1026 1000		1105 1006	ν_3 antisymmetric stretching mode of VO_4
899		927 903	943	994 948		912 911	
846 842		846			885 874		ν_1 symmetric stretching mode of VO_4
769	810	787	809	800		797	
736 677	674 644		672 641		707 643	743	ν_3 antisymmetric stretching mode of VO_4
563							
410	493 412		498 410		465 413 404		ν_4 bending modes of VO_4 units
370	340		341		370		ν_2 bending

328					348 331		modes of VO_4 units
288 247 212	259 249		248 197		264 204 185		Lattice modes

List of Figures

Figure 1 Raman spectra of pucherite, namibite, schumacherite, pottsite and clinobisvanite in the 750 to 950 cm^{-1} region.

Figure 2 Raman spectra of pucherite, namibite, schumacherite, pottsite and clinobisvanite in the 750 to 250 cm^{-1} region.

Figure 3 Raman spectra of namibite, schumacherite, pottsite and clinobisvanite in the 4000 to 2500 cm^{-1} region.

Figure 4 Infrared spectra of pucherite, namibite, schumacherite, pottsite and clinobisvanite in the 4000 to 2500cm^{-1} region.

Figure 5 Infrared spectra of pucherite, namibite, schumacherite, pottsite and clinobisvanite in the 1500 to 500 cm^{-1} region.

List of Tables

Table 1 Samples, museum reference and origin of the $BiVO_4$ samples

Table 2 Results of the Raman and infrared spectral analysis of pucherite and clinobisvanite.

Table 3 Results of the Raman and infrared spectral analysis of namibite, schumacherite and pottsite.

Figure 1

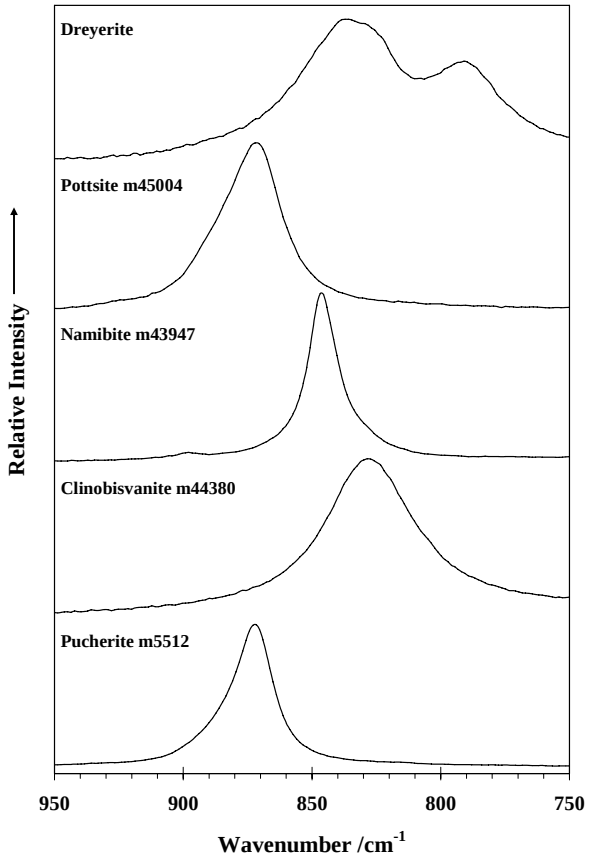
Dreyerite
Pottsite m45004
Namibite m43947
Clinobisvanite m44380
Pucherite m5512
Relative Intensity
950
900
850
800
750
Wavenumber /cm-1

Figure 2

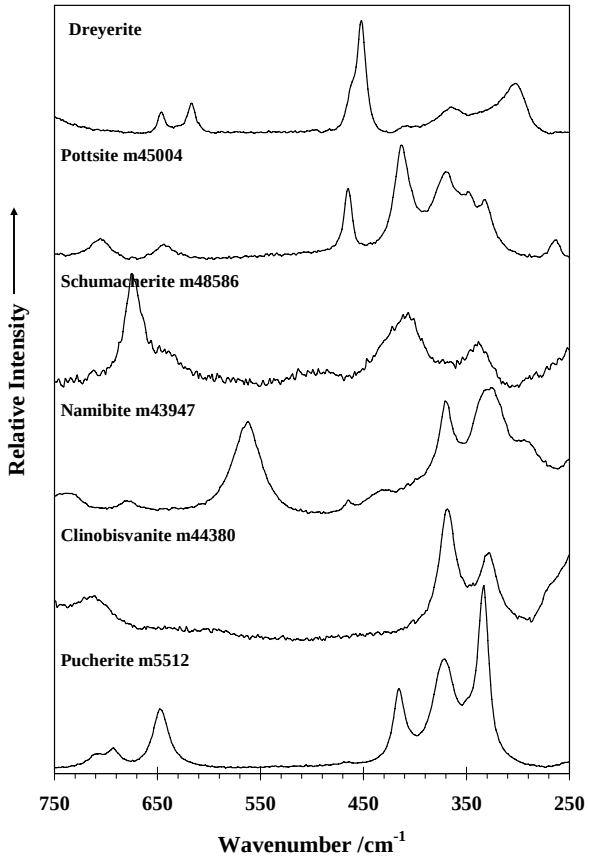
Dreyerite
Pottsite m45004
Schumacherite m48586
Namibite m43947
Clinobisvanite m44380
Pucherite m5512
Relative Intensity
750
650
550
450
350
250
Wavenumber /cm-1

Figure 3

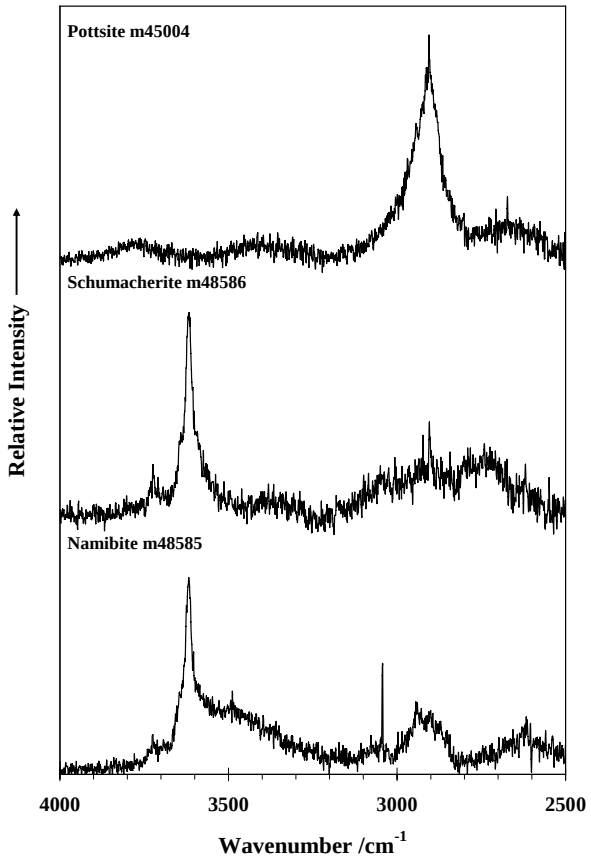
Pottsite m45004
Schumacherite m48586
Namibite m48585
Relative Intensity
4000
3500
3000
2500
Wavenumber /cm-1

Figure 4

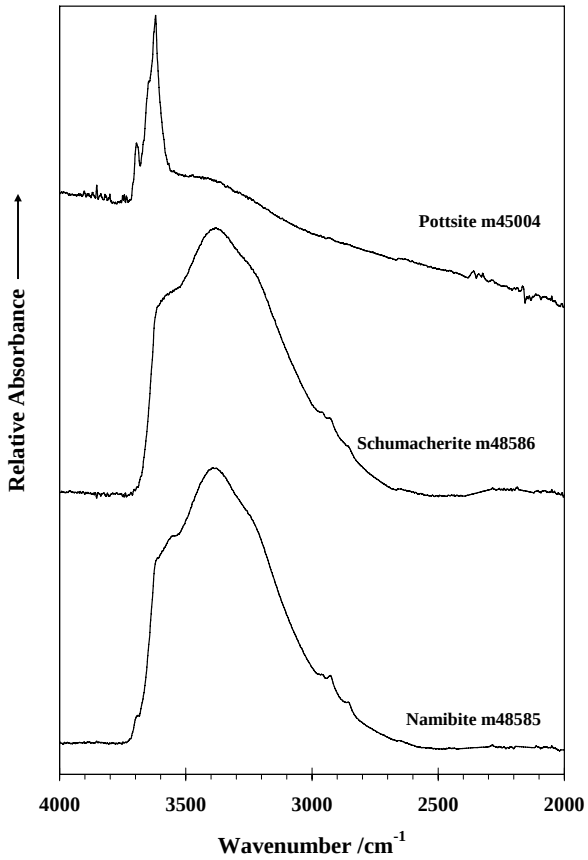
Pottsite m45004
Schumacherite m48586
Namibite m48585
Relative Absorbance
4000
3500
3000
2500
2000
Wavenumber /cm-1

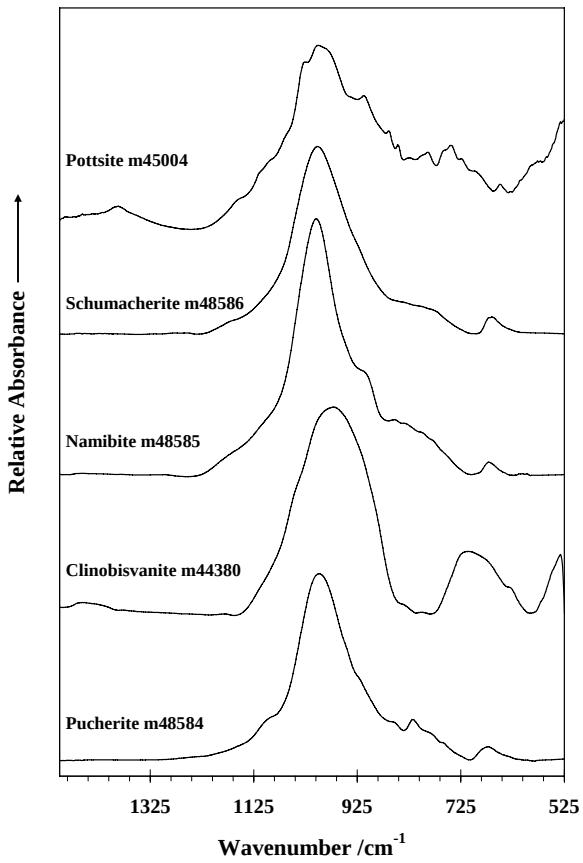
Pottsite m45004
Schumacherite m48586
Namibite m48585
Clinobisvanite m44380
Pucherite m48584
Relative Absorbance
1325
1125
925
725
525
Wavenumber /cm-1

Figure 5